

THF solution) and was followed after addition of hexane (equal volume) by slow (12 h) deposition of bright yellow crystals. This product was shown by using X-ray diffractometry⁸ to be the binuclear complex $\text{Ru}_2(\text{CO})_3(\text{OCOCF}_3)(\mu\text{-OSiMe}_2\text{CH}_2\text{PPh}_2)_2(\mu\text{-OCOCF}_3)$ (**4**): the molecular structure is illustrated in Figure 1. Simultaneously it was discovered that synthesis⁶ of complex **2** by action of $\text{CF}_3\text{CO}_2\text{H}$ on $[\text{Ru}(\text{CO})_3(\mu\text{-SiMe}_2\text{CH}_2\text{PPh}_2)]_2$ (**5**) is accompanied by formation of a minor constituent (<10%), which was obtained as colorless crystals: this was identified as $[\text{Ru}(\text{CO})_2(\text{OCOCF}_3)(\mu\text{-OSiMe}_2\text{CH}_2\text{PPh}_2)]_2$ (**6**) (also by X-ray structure determination,⁹ see Figure 2), a potential precursor to **4**. Accordingly UV irradiation of **6** (THF solution) rapidly (5 min) affords **4**, although no **6** was observed after exposure of **4** to CO (18 h, ca. 800 psig).

The asymmetric structure of compound **4**, which is evident from the NMR data⁸ (diastereotopic methyl groups and methylene hydrogens), is derived from that of **6** by entry of a terminal ester group to displace CO at the second Ru center, forming an unsymmetrical bridge to the latter (Ru-O = 2.12, 2.18 Å; cf. 2.09 Å to the residual terminal ester). Smaller differences in Ru-O distances to the bridging siloxyl fragments compensate one another (2.09, 2.14 vs 2.11, 2.09 Å), and the overall geometry is consistent with formal Ru(II) character for both metal atoms, a conclusion

that is self-evident in the structure of **6** under the constraints of crystallographic symmetry. The Ru₂ distances of 3.247 (**4**) and 3.313 Å (**6**) both lie outside bonding range; i.e. the molecules model "broken-up" Ru clusters on a silica surface.⁴ Most significantly, the Ru-O distances (2.14 Å, **6**; mean 2.11 Å, **4**) confirm that the estimate¹⁰ of 2.17 Å from EXAFS data for a decomposed ruthenium cluster on alumina is essentially correct, reinforce the assertion⁴ that "EXAFS results are in agreement with those obtained from X-ray diffraction", and imply directly that in catalytically active surface entities formed by attachment of Ru(0) at an oxide support "the oxidation state of the ruthenium atoms...is different from zero".⁴ Further investigation of relationships between complexes **2-6** is in progress (in particular formation of **4** from **2**, which appears to involve dimerization of a reactive mononuclear species as projected above and parallels the role of surface Si-OH in formation of oxidized metal centers¹¹); it is anticipated that attachment of alkyl or alkenyl ligands at Ru in these new systems will provide information on how the chemistry of hydrocarbon assembly¹² is influenced by electronic characteristics of the oxide surface.

Acknowledgment. We thank the NSERC for financial support, including an infrastructure grant for X-ray crystallography, and K. A. Beveridge, R. D. Brost, and Dr. G. W. Bushnell for assisting with the structure determinations.

Supplementary Material Available: For compounds **4** and **6**, tables of crystallographic parameters, fractional atomic coordinates, temperature parameters, and bond distances and angles (9 pages); tables of structure factors (21 pages). Ordering information is given on any current masthead page.

(8) Crystal data for compound **4**: $\text{C}_{37}\text{H}_{36}\text{F}_6\text{O}_9\text{P}_2\text{Ru}_2\text{Si}_2$; $M_r = 1058.9$; triclinic; space group $P\bar{1}$; $a = 9.166$ (2) Å, $b = 13.718$ (2) Å, $c = 18.096$ (3) Å; $\alpha = 110.73$ (3)°, $\beta = 90.50$ (2)°, $\gamma = 94.73$ (2)°; $V = 2119$ Å³; $Z = 2$; D_{calc} = 1.67 g cm⁻³; Nonius CAD4 diffractometer; Mo Kα ($\lambda = 0.71069$ Å) radiation, $\mu = 8.19$ cm⁻¹; 4818 unique reflections refined to a conventional $R = 0.070$ ($R_w = 0.073$). Selected spectroscopic data are as follows. IR (cm⁻¹): 2065, 2000, 1952 (ν_{CO}); 1690, 1650 ($\nu_{\text{C-O(ester)}}$). ¹H NMR (CDCl₃ solution, δ vs TMS): -0.03 (s, 3 H), 0.03 (s, 3 H), 0.17 (s, 3 H), 0.36 (s, 3 H), 1.50 (t, 1 H), 1.63 (t, 1 H), 1.73 (t, 1 H), 1.87 (t, 1 H), 7.3-7.8 (m, 20 H). ³¹P NMR (CDCl₃ solution, δ vs TMP): -77.7 (s), -93.5 (s).

(9) Crystal data for compound **6**: $\text{C}_{38}\text{H}_{36}\text{F}_6\text{O}_{10}\text{P}_2\text{Ru}_2\text{Si}_2$; $M_r = 1086.9$; monoclinic; space group $P2_1/n$; $a = 12.696$ (6) Å, $b = 15.320$ (5) Å, $c = 11.343$ (5) Å; $\beta = 92.31$ (3)°; $V = 2205$ Å³; $Z = 2$; D_{calc} = 1.64 g cm⁻³; Nonius CAD4 diffractometer; Mo Kα ($\lambda = 0.71069$ Å) radiation, $\mu = 8.47$ cm⁻¹; 1262 unique reflections refined to a conventional $R = 0.060$ ($R_w = 0.057$). Selected spectroscopic data are as follows. IR (cm⁻¹): 2065, 2001 (ν_{CO}); 1687 ($\nu_{\text{C-O(ester)}}$). ¹H NMR (CDCl₃ solution, δ vs TMS): 0.26 (s, 3 H), 0.52 (s, 3 H), 1.65 (t, 1 H), 2.02 (t, 1 H), 7.3-7.8 (m, 10 H). ³¹P NMR (CDCl₃ solution, δ vs TMP): -87.9.

(10) Asakura, K.; Yamada, M.; Iwasawa, Y.; Kuroda, H. *Chem. Lett.* **1985**, 511.

(11) Basu, P.; Panayotov, D.; Yates, J. T. *J. Am. Chem. Soc.* **1988**, *110*, 2074.

(12) See for example: Knox, S. A. R. *Pure Appl. Chem.* **1984**, *56*, 81 and references therein.

Department of Chemistry
University of Victoria
Victoria, British Columbia,
Canada V8W 2Y2

Gregg C. Bruce
Stephen R. Stobart*

Received July 22, 1988

Articles

Contribution from the Department of Chemistry and Biochemistry,
University of Arkansas, Fayetteville, Arkansas 72701

(Polypyridine)ruthenium(II) Complexes Containing Sulfite, Bisulfite, and Sulfur Dioxide

L. R. Allen, D. Y. Jeter, A. W. Cordes, and B. Durham*

Received February 29, 1988

Complexes of the type $\text{Ru}(\text{bpy})_2(\text{HSO}_3)\text{L}$, where L is bisulfite, water, and pyridine, have been prepared and the acid-base equilibria of coordinated bisulfite examined. For L = pyridine or water a single equilibrium is observed ($\text{p}K = 3.7$ in both cases), which corresponds to the bisulfite/sulfite equilibrium. Evidence for the presence of the sulfur dioxide complex is observed only in 6 M H_2SO_4 . These data indicate that sulfur dioxide coordinated to the $\text{Ru}(\text{bpy})_2$ moiety is significantly more electrophilic than in the polyamine complexes of ruthenium(II). The complex in which L is bisulfite crystallizes in the monoclinic $P2_1/n$ space group with $a = 9.008$ (1) Å, $b = 21.380$ (4) Å, $c = 11.151$ (1) Å, $\alpha = 96.02$ (1)°, and $Z = 4$. When L is pyridine, the crystals are triclinic, $P\bar{1}$, with $a = 9.767$ (2) Å, $b = 10.785$ (1) Å, $c = 17.626$ (5) Å, $\alpha = 69.29$ (2)°, $\beta = 71.41$ (2)°, $\gamma = 65.64$ °, and $Z = 2$. The respective numbers of observed reflections were 1512 and 3737, R 's were 0.050 and 0.058, and R_w 's were 0.053 and 0.071.

Introduction

The similarities in the ligating properties of nitric oxide and sulfur dioxide have been well documented in the last two decades.¹

Both of these ligands exhibit at least two different geometries when coordinated, and the preferred geometry appears to depend on the number of d electrons in a similar manner. The tetra- and pentaammine complexes of ruthenium² have been particularly

(1) (a) Ryan, R. R.; Eller, P. G. *Inorg. Chem.* **1976**, *15*, 494. (b) Bottemley, F. *Acc. Chem. Res.* **1978**, *11*, 158.

(2) Brown, G. M.; Sutton, J. E.; Taube, H. *J. Am. Chem. Soc.* **1978**, *100*, 2767.

useful in the study of these properties and are continuing to receive attention. Meyer and co-workers,³ among others, have extended the work to the bipyridine complexes of ruthenium(II). Interestingly, sulfur dioxide complexes of ruthenium(II) containing bipyridine ligands are conspicuously absent from the literature.

The following describes an investigation of the chemistry of complexes containing sulfite, bisulfite, and sulfur dioxide coordinated to the bis(bipyridine)ruthenium(II) moiety. No sulfur dioxide complexes have been isolated as solids. This fact, along with the absence of such complexes from the literature, is readily explained by the solution chemistry of complexes that contain coordinated bisulfite. The synthesis, structure, and solution chemistry of these complexes form the basis of this report.

Experimental Section

Materials and Supplies. Ru(bpy)₂Cl₂ and [Ru(bpy)₂(py)Cl]PF₆ (bpy = 2,2'-bipyridine; py = pyridine) were prepared according to published procedures.⁴ All other chemicals were reagent grade and were used as received.

Equipment. Visible absorption data were collected with a Cary 14 spectrophotometer, and IR data were obtained with a Perkin-Elmer 283 IR spectrometer. Cyclic voltammetry was performed with equipment built in our laboratory and has been previously described.⁵ A platinum-bead electrode was used as the working electrode and a platinum wire as the auxiliary electrode. The reference was a saturated sodium chloride calomel electrode. Cyclic voltammetry was performed in 0.1 M tetrabutylammonium hexafluorophosphate/acetonitrile solution. An Orion 601A digital ionalyzer was used for the pH measurements.

cis-[Ru(bpy)₂(HSO₃)₂]-H₂O. Excess sodium sulfite (1.0 g, 8 mmol) was added to 40 mL of an aqueous solution of *cis*-Ru(bpy)₂Cl₂·2H₂O (0.30 g, 0.6 mmol). The solution was heated for 1 h and allowed to cool to room temperature. The addition of 2 mL of concentrated hexafluorophosphoric acid caused the solution to become cloudy. The amount of acid added is very important and dramatically affects the yield. The product was recovered after 2 h by vacuum filtration, washed with cold 2-propanol and then ethyl ether, and air-dried. Additional product was recovered from the filtrate by reducing the volume by rotary evaporation and repeating the workup. The yield was 0.23 g, 67%. Yellow crystals suitable for structure determination were grown by adding HPF₆ while the reaction mixture was still warm and then allowing the solution to cool slowly. Anal. Calcd for RuC₂₀H₂₂N₄S₂O₆: C, 39.28; H, 3.63; N, 9.16; S, 10.48. Found: C, 39.61; H, 3.51; N, 9.11; S, 10.04.

cis-[Ru(bpy)₂(HSO₃)(H₂O)]PF₆. More than 1 equiv of sodium sulfite (0.040 g, 0.31 mmol) was added to a solution of *cis*-Ru(bpy)₂Cl₂ (0.12 g, 0.23 mmol) in 30 mL of 0.1 N H₂SO₄ after boiling under N₂ for 5 min. The solution was stirred at room temperature for 1 h, and 1 mL of concentrated hexafluorophosphoric acid was added. The extent of reaction was monitored by visible spectroscopy and was judged complete when no trace of a 480-nm shoulder (due to Ru(bpy)₂(H₂O)₂²⁺) was evident. The solution was concentrated by evaporation under vacuum at room temperature to 15 mL. Precipitation was allowed to proceed 12 h in the refrigerator after the reduction in volume. The dark red solid was recovered by vacuum filtration, washed with 2-propanol and diethyl ether, and air-dried. The yield was 0.040 g, 26%. Anal. Calcd for RuC₂₀H₁₉N₄O₄SPF₆: C, 36.54; H, 2.91; N, 8.52; S, 4.87. Found: C, 37.16; H, 2.70; N, 8.71; S, 4.99.

cis-[Ru(bpy)₂(HSO₃)(py)]PF₆·H₂O. An aqueous solution of *cis*-[Ru(bpy)₂(py)Cl]PF₆ (0.080 g in 30 mL) was heated to boiling under N₂ for 5 min. After the mixture was cooled for 10 min, excess sodium sulfite was added (0.7 g, 5.6 mmol). The color of the solution changed slowly to orange. After 15 min, the solution was filtered and 1 mL of concentrated hexafluorophosphoric acid added to the liquid. The resulting precipitate was collected by vacuum filtration, washed with 2-propanol and then diethyl ether, and air-dried. The yield was 0.061 g, 71%. Yellow crystals suitable for structure determination were grown by slow evaporation of an 0.1 N H₂SO₄ solution of the complex containing a small amount of hydroquinone. Anal. Calcd for RuC₂₅H₂₄N₅O₄SPF₆: C, 40.76; H, 3.28; N, 9.50. Found: C, 40.66; H, 3.17; N, 9.55.

Determination of Equilibrium Constants. The equilibrium constants for the equilibria involving coordinated bisulfite were determined by

Table I. Visible Absorption Maxima of Ru(bpy)₂LL' in 0.1 N H₂SO₄ with NaOH Added To Adjust pH to Indicated Value

L, L'	abs max, nm	pH	L, L'	abs max, nm	pH
(SO ₂) ₂	... ^a		SO ₂ , H ₂ O	398	-0.8
SO ₂ , HSO ₃	365	0	HSO ₃ , H ₂ O	416	1
(HSO ₃) ₂	...		SO ₃ , H ₂ O	456	8
HSO ₃ , SO ₃	392	4	SO ₂ , py	...	
(SO ₃) ₂	425	10	HSO ₃ , py	404	1
			SO ₃ , py	444	8

^aThe leaders indicate conditions could not be found under which a reliable measurement could be obtained.

Table II. Equilibrium Constants for *cis*-Ru(bpy)₂LL' Determined by Spectrophotometric Titration of the Appropriate Bisulfite Complex in Phosphate Buffer

L, L'	pK	L, L'	pK
HSO ₃ , H ₂ O/SO ₃ , H ₂ O	3.7	SO ₂ , SO ₂ /HSO ₃ , HSO ₃	2.0 ^a
HSO ₃ , py/SO ₃ , py	3.7	HSO ₃ , HSO ₃ /HSO ₃ , SO ₃	8.8

^aApproximately (pK₁pK₂)^{1/2}; see text.

Table III. Crystallographic Data

[Ru(bpy) ₂ (HSO ₃) ₂]-H ₂ O	
RuS ₂ O ₇ N ₄ C ₂₀ H ₂₀	fw: 593.6
<i>a</i> = 9.008 (1) Å	space group: P2 ₁ /n
<i>b</i> = 21.380 (4) Å	<i>T</i> = 20 °C
<i>c</i> = 11.151 (1) Å	λ = 0.71073 Å
β = 96.02 (1)°	ρ _{calc} = 1.85 g cm ⁻³
<i>V</i> = 2135.7 (9) Å ³	μ = 9.6 cm ⁻¹
<i>Z</i> = 4	transmission coeff = 0.96-1.00
	<i>R</i> (<i>F</i> _o) = 0.050
	<i>R</i> _w (<i>F</i> _o) = 0.053
[Ru(bpy) ₂ (py)(HSO ₃)]PF ₆ ·3H ₂ O	
RuPSF ₆ O ₆ N ₅ C ₂₅ H ₂₈	fw: 772.6
<i>a</i> = 9.767 (2) Å	space group: P1̄
<i>b</i> = 10.785 (1) Å	<i>T</i> = 20 °C
<i>c</i> = 17.626 (5) Å	λ = 0.71073 Å
α = 69.29 (2)°	ρ _{calc} = 1.66 g cm ⁻³
β = 71.41 (2)°	μ = 7.1 cm ⁻¹
γ = 65.64 (1)°	transmission coeff = 0.93-1.00
<i>V</i> = 1549.1 Å ³	<i>R</i> (<i>F</i> _o) = 0.058
<i>Z</i> = 2	<i>R</i> _w (<i>F</i> _o) = 0.071

spectrophotometric titrations of the complexes. Typically, 50 mL of a stock solution of complex in 0.05 M phosphate buffer⁶ with 20 mg of hydroquinone was titrated with H₂SO₄ solutions with concentrations such that 1 or 2 drops of solution was sufficient to alter the pH of the solution under observation by 0.2-0.5 pH unit. The concentration of titrant was changed throughout the titration in order to avoid a significant dilution error. After each addition, the pH was determined and the absorbance of a 3-mL aliquot was measured at two or three different wavelengths. The aliquot was returned to the reaction solution. The absorbance changes due to dilution were assessed at wavelengths unaffected by the titration and deemed sufficiently small to neglect. The values of the equilibrium constants were determined by best fits to plots of pH versus the change in absorbance divided by the total change in absorbance for the entire titration at a particular wavelength. The best fits were determined by visual comparison to computer-generated plots of ideal cases. This fitting procedure results in a standard deviation of the pK_a's of approximately 0.1. The pH meter was calibrated with three standard buffer solutions at pH values of 1.0, 4.0, and 7.2.

X-ray Structure Determinations. Table III summarizes the crystallographic and refinement data. The intensities were measured with an Enraf-Nonius CAD-4 diffractometer using ω-2θ scans of 4-16° min⁻¹ in θ for reflections to 2θ of 50° and Mo Kα X-rays (graphite monochromator). Unit cells were determined from a least-squares analysis of angle data for 25 reflections with 16 < 2θ < 22°.

Both structures were solved by Patterson and Fourier methods, and the full-matrix least squares minimized Σw(Δ*F*)² with non-Poisson w⁻¹

- Godwin, J. B.; Meyer, T. J. *Inorg. Chem.* **1971**, *10*, 471. Callahan, R. W.; Meyer, T. J. *Inorg. Chem.* **1977**, *16*, 574.
- Durham, B.; Walsh, J. L.; Carter, C. L.; Meyer, T. J. *Inorg. Chem.* **1980**, *19*, 860.
- Woodward, W. S.; Rocklin, R. D.; Murray, R. W. *Chem., Biomed. Environ. Instrum.* **1979**, *9*, 25.

- Phosphate buffer No. 2 in: Gordon, A. J.; Ford, R. A. *The Chemist's Companion: A Handbook of Practical Data, Techniques, and References*; Wiley-Interscience: New York, 1972.

Table IV. Selected Interatomic Distances (Å) and Angles (deg)

[Ru(bpy) ₂ (HSO ₃)(py)]PF ₆ ·3H ₂ O		Ru(bpy) ₂ (HSO ₃) ₂ ·H ₂ O	
Ru-S	2.286 (2)	Ru-S(1)	2.288 (4)
		Ru-S(2)	2.298 (4)
S-O(1)	1.465 (5)	S(1)-O(1)	1.460 (10)
S-O(2)	1.586 (5)	S(1)-O(2)	1.587 (10)
S-O(3)	1.469 (5)	S(1)-O(3)	1.444 (11)
		S(2)-O(4)	1.476 (8)
		S(2)-O(5)	1.612 (8)
		S(2)-O(6)	1.446 (10)
Ru-N(1)	2.089 (5)	Ru-N(1)	2.080 (10)
Ru-N(2)	2.066 (5)	Ru-N(2)	2.096 (11)
Ru-N(3)	2.073 (5)	Ru-N(3)	2.092 (11)
Ru-N(4)	2.090 (6)	Ru-N(4)	2.081 (11)
Ru-N(5)	2.108 (5)		
O(1)-S-O(2)	105.3 (3)	O(1)-S(1)-O(2)	105.6 (7)
O(1)-S-O(3)	109.6 (3)	O(1)-S(1)-O(3)	110.5 (8)
O(2)-S-O(3)	101.5 (3)	O(2)-S(1)-O(3)	99.7 (6)
		O(4)-S(2)-O(5)	103.0 (5)
		O(4)-S(2)-O(6)	111.6 (6)
		O(5)-S(2)-O(6)	102.6 (5)
		S(1)-Ru-S(2)	93.5 (2)
S-Ru-N(1)	101.1 (2)	S(1)-Ru-N(1)	87.6 (3)
S-Ru-N(2)	94.0 (2)	S(1)-Ru-N(2)	90.9 (3)
S-Ru-N(3)	85.6 (2)	S(1)-Ru-N(3)	101.1 (3)
S-Ru-N(4)	178.7 (2)	S(1)-Ru-N(4)	176.3 (3)
S-Ru-N(5)	91.3 (2)		
		S(2)-Ru-N(1)	95.9 (3)
		S(2)-Ru-N(2)	172.9 (3)
		S(2)-Ru-N(3)	91.7 (3)
		S(2)-Ru-N(4)	90.0 (5)
N(1)-Ru-N(2)	95.7 (2)	N(1)-Ru-N(2)	78.6 (4)
N(2)-Ru-N(3)	78.2 (2)	N(2)-Ru-N(3)	92.9 (4)
N(1)-Ru-N(3)	171.3 (2)	N(1)-Ru-N(3)	168.0 (4)
N(2)-Ru-N(4)	85.8 (2)	N(2)-Ru-N(4)	85.8 (4)
N(1)-Ru-N(4)	77.7 (2)	N(1)-Ru-N(4)	93.5 (4)
N(3)-Ru-N(4)	95.6 (2)	N(3)-Ru-N(4)	77.2 (4)
N(1)-Ru-N(5)	87.9 (2)		
N(2)-Ru-N(5)	172.9 (2)		
N(3)-Ru-N(5)	97.6 (2)		
N(4)-Ru-N(5)	89.0 (2)		

$= [\sigma^2(I) + 0.0025I^2]/4F^2$ to a final $(\Delta/\sigma)_{\max} < 0.01$. No extinction parameter was included. The H atoms of the bpy and py ligands were constrained to idealized (C-H = 0.95 Å) positions with isotropic $B = 1.2B$ of the bonded C atom. The bisulfite H atoms were constrained to positions found on difference maps. All non-H atoms were refined anisotropically, except for the O atom of the water in structure I and the disordered F atoms (two octahedra of populations 0.6 and 0.4) of the PF₆⁻ anion in structure II. Atomic scattering factors and anomalous dispersion corrections were taken from ref 16, and the programs used were those of the Enraf-Nonius SDP programs (1982). Table V gives the atom coordinates and Table IV selected distances and angles. Figures 4 and 5 show the molecules with the numbering schemes.

Results and Discussion

The synthesis of the complexes of interest followed procedures similar to those published^{3,4} for many ruthenium(II) complexes containing bipyridine ligands. The nature of the reactions, the inability to produce complexes containing coordinated SO₂, and the instability of the complexes produced show a great divergence, however, from the chemistry normally observed with this family of compounds.

Ru(bpy)₂(HSO₃)₂. *cis*-Ru(bpy)₂(HSO₃)₂ was prepared by the reaction of *cis*-Ru(bpy)₂(H₂O)₂²⁺ (generated from the dichloro complex) with excess bisulfite ion. The reaction with bisulfite ion is extremely rapid, being essentially complete within the time of mixing when the reaction is carried out at concentrations suitable for spectrophotometric monitoring. Preliminary kinetics studies indicate that the reaction is not a simple substitution reaction. Addition of hydroquinone, for example, at pH 2 reduces the observed rate constant for the formation of products by several orders of magnitude. The reduction in rate by hydroquinone

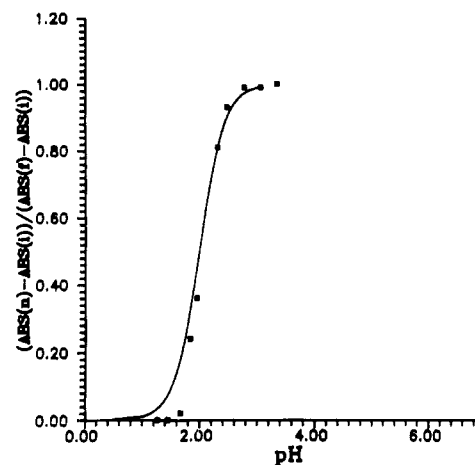
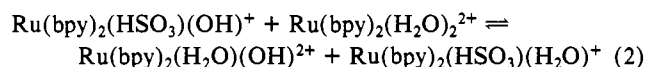
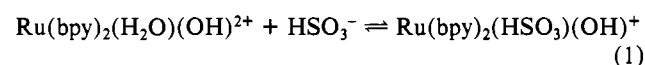


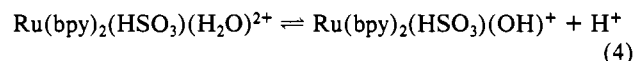
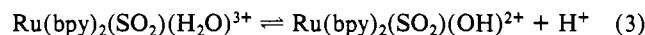
Figure 1. Spectrophotometric titration of Ru(bpy)₂(HSO₃)₂ over the range of pH 0–5.

suggests catalysis by higher oxidation state species⁷ such as those indicated in reactions 1 and 2. Reactions such as (2) are typically



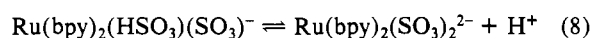
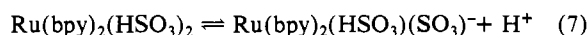
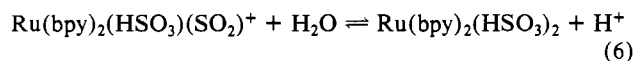
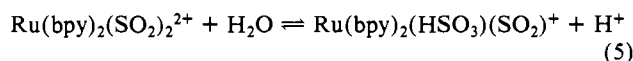
very rapid with ruthenium(II) complexes of bipyridine.⁸ Reaction 1 may involve direct attack of bisulfite or metabisulfite ion on the coordinated OH, followed by rearrangement to the S-bound isomer. In this case, cleavage of a Ru–O bond would not be the rate-limiting process. The rate of substitution without added hydroquinone shows a strong pH dependence over the range of 0–4 in keeping with the above scheme.

The extent of the reaction of Ru(bpy)₂(H₂O)₂²⁺ with bisulfite ion is also pH-dependent. If the catalysis scheme suggested by reactions 1 and 2 is correct, then the pH dependence can be readily rationalized in terms of an increase of the pK_a of the coordinated water in the monosubstituted derivatives of Ru(III):



At pH > 3 and with no added hydroquinone, the reaction proceeds to the disubstituted complex with no indication of an intermediate step even on the time scale of stopped-flow mixing. At pH 1 and with no added hydroquinone, the reaction proceeds with isosbestic points to a product that has an absorbance maximum at 416 nm. The disubstituted complex shows a maximum at 365 nm at this pH. The product can be isolated and is *cis*-[Ru(bpy)₂(H₂O)(HSO₃)]PF₆.

Once the disubstituted complex is formed, it is stable for a period of at least several hours over the range of pH 1–10. The stability of the disubstituted species allowed the determination of the equilibrium constants of reactions 5–8. These were de-



(7) Chang, J.; Meyerhoffer, S.; Allen, L. R.; Durham, B.; Walsh, J. L. *Inorg. Chem.* **1988**, *27*, 1602.

(8) *Inorganic and Organometallic Photochemistry*; Wrighton, M., Ed.; Advances in Chemistry 168; American Chemical Society: Washington, DC, 1978.

Table V. Fractional Atomic Coordinates and Isotropic Thermal Parameters^a

atom	x	y	z	B_{eq} or $B, \text{\AA}^2$	atom	x	y	z	B_{eq} or $B, \text{\AA}^2$
A. $\text{Ru}(\text{bpy})_2(\text{HSO}_3)_2 \cdot \text{H}_2\text{O}$									
Ru	0.1798 (1)	0.10618 (5)	-0.19980 (9)	1.40 (2)	C(4)	0.638 (1)	0.1557 (7)	-0.067 (1)	3.0 (3)
S(1)	0.1214 (4)	0.1129 (2)	-0.0055 (3)	2.56 (7)	C(5)	0.508 (1)	0.1227 (6)	-0.094 (1)	2.0 (3)
S(2)	0.2689 (3)	0.0058 (2)	-0.1757 (3)	1.88 (7)	C(6)	0.238 (1)	0.2419 (6)	-0.215 (1)	2.1 (3)
O(1)	-0.012 (1)	0.0791 (6)	0.0204 (8)	4.9 (3)	C(7)	0.220 (2)	0.3042 (7)	-0.242 (1)	3.0 (3)
O(2)	0.254 (1)	0.0844 (5)	0.0829 (8)	3.7 (2)	C(8)	0.078 (2)	0.3255 (6)	-0.285 (1)	2.7 (3)
O(3)	0.120 (1)	0.1758 (5)	0.0415 (9)	5.1 (3)	C(9)	-0.037 (2)	0.2852 (7)	-0.300 (1)	3.5 (4)
O(4)	0.3272 (9)	-0.0100 (4)	-0.0507 (8)	2.5 (2)	C(10)	-0.010 (1)	0.2239 (6)	-0.271 (1)	1.9 (3)
O(5)	0.1394 (8)	-0.0455 (4)	-0.2068 (8)	1.8 (2)	C(11)	-0.032 (1)	0.0769 (6)	-0.411 (1)	1.7 (3)
O(6)	0.375 (1)	-0.0095 (5)	-0.2599 (9)	3.5 (2)	C(12)	-0.166 (2)	0.0629 (7)	-0.480 (1)	2.9 (3)
O(7)	0.156 (2)	0.294 (1)	0.069 (2)	8.9 (5)*	C(13)	-0.286 (1)	0.0444 (6)	-0.427 (1)	3.3 (3)
N(1)	0.381 (1)	0.1501 (5)	-0.1422 (9)	2.0 (2)	C(14)	-0.278 (1)	0.0398 (7)	-0.303 (1)	2.8 (3)
N(2)	0.124 (1)	0.2004 (5)	-0.2299 (9)	1.8 (2)	C(15)	-0.142 (1)	0.0544 (6)	-0.237 (1)	2.6 (3)
N(3)	-0.022 (1)	0.0746 (5)	-0.2886 (9)	2.1 (2)	C(16)	0.102 (1)	0.0933 (6)	-0.464 (1)	2.0 (3)
N(4)	0.223 (1)	0.1046 (5)	-0.3796 (8)	1.8 (2)	C(17)	0.120 (1)	0.0959 (6)	-0.584 (1)	1.9 (3)
C(1)	0.384 (1)	0.2116 (7)	-0.167 (1)	2.7 (3)	C(18)	0.254 (2)	0.1114 (7)	-0.625 (1)	3.0 (3)
C(2)	0.513 (2)	0.2474 (7)	-0.146 (1)	4.1 (4)	C(19)	0.376 (2)	0.1250 (7)	-0.540 (1)	3.3 (4)
C(3)	0.642 (2)	0.2173 (8)	-0.096 (2)	4.4 (4)	C(20)	0.356 (1)	0.1210 (6)	-0.420 (1)	2.3 (3)
B. $[\text{Ru}(\text{bpy})_2(\text{py})(\text{HSO}_3)]\text{PF}_6 \cdot 3\text{H}_2\text{O}$									
Ru	0.12258 (6)	0.08678 (6)	0.23033 (3)	2.52 (1)	C(2)	-0.3103 (9)	0.0050 (9)	0.3249 (6)	5.0 (3)
S(1)	0.0266 (2)	0.1967 (2)	0.1118 (1)	3.38 (5)	C(3)	-0.2688 (9)	-0.1367 (9)	0.3658 (6)	5.8 (3)
P	0.3340 (3)	0.4370 (2)	0.3777 (1)	5.00 (7)	C(4)	-0.1157 (9)	-0.2130 (8)	0.3645 (5)	4.4 (2)
F(1)	0.245 (1)	0.494 (1)	0.3021 (7)	8.7 (3)*	C(5)	-0.0109 (7)	-0.1455 (7)	0.3251 (4)	3.3 (2)
F(2)	0.198 (1)	0.562 (1)	0.4153 (6)	7.9 (3)*	C(6)	0.2518 (9)	-0.1670 (8)	0.1564 (5)	4.3 (2)
F(3)	0.392 (1)	0.560 (1)	0.3091 (8)	10.2 (4)*	C(7)	0.364 (1)	-0.2628 (8)	0.1153 (5)	5.4 (3)
F(4)	0.410 (1)	0.384 (1)	0.4538 (7)	8.2 (3)*	C(8)	0.506 (1)	-0.2542 (9)	0.0851 (6)	7.1 (3)
F(5)	0.486 (1)	0.327 (1)	0.3410 (6)	7.8 (3)*	C(9)	0.535 (1)	-0.147 (1)	0.0951 (6)	6.2 (3)
F(6)	0.283 (2)	0.323 (2)	0.4506 (9)	13.3 (5)*	C(10)	0.4199 (9)	-0.0515 (8)	0.1351 (5)	3.9 (2)
F(7)	0.164 (2)	0.460 (1)	0.4417 (9)	6.7 (3)*	C(11)	0.4371 (8)	0.0708 (8)	0.1446 (5)	3.8 (2)
F(8)	0.441 (1)	0.455 (1)	0.4288 (7)	4.8 (3)*	C(12)	0.5717 (9)	0.104 (1)	0.1153 (6)	5.6 (3)
F(9)	0.314 (2)	0.589 (2)	0.368 (1)	9.0 (5)*	C(13)	0.5743 (9)	0.2216 (9)	0.1254 (6)	5.5 (3)
F(10)	0.492 (2)	0.399 (1)	0.3114 (9)	7.3 (4)*	C(14)	0.4474 (9)	0.3076 (8)	0.1642 (5)	4.8 (2)
F(11)	0.764 (1)	0.571 (1)	0.6741 (8)	5.9 (3)*	C(15)	0.3170 (8)	0.2708 (7)	0.1930 (5)	3.9 (2)
F(12)	0.327 (2)	0.281 (2)	0.388 (1)	8.7 (4)*	C(16)	0.3135 (8)	-0.1383 (8)	0.3574 (5)	3.8 (2)
O(1)	-0.1113 (6)	0.3221 (6)	0.1140 (3)	4.6 (2)	C(17)	0.3682 (8)	-0.1971 (8)	0.4293 (5)	4.3 (2)
O(2)	0.1513 (6)	0.2481 (5)	0.0381 (3)	4.3 (2)	C(18)	0.313 (1)	-0.116 (1)	0.4851 (5)	5.4 (3)
O(3)	0.0033 (7)	0.0992 (5)	0.0803 (3)	5.7 (2)	C(19)	0.205 (1)	0.0138 (9)	0.4694 (5)	5.0 (2)
O(4)	0.1815 (7)	0.4792 (6)	0.0317 (4)	5.6 (2)	C(20)	0.1518 (7)	0.0665 (7)	0.3958 (4)	3.2 (2)
O(5)	-0.0755 (7)	-0.1275 (6)	0.0919 (4)	6.0 (2)	C(21)	0.0321 (7)	0.2004 (7)	0.3749 (4)	3.4 (2)
O(6)	0.058 (1)	0.6014 (8)	0.1674 (5)	9.8 (3)	C(22)	-0.0445 (9)	0.2934 (8)	0.4257 (5)	4.5 (2)
N(1)	-0.0065 (6)	0.2339 (6)	0.3002 (4)	3.3 (1)	C(23)	-0.158 (1)	0.4154 (8)	0.4019 (5)	5.1 (2)
N(2)	0.3084 (6)	0.1564 (6)	0.1828 (3)	3.2 (2)	C(24)	-0.199 (1)	0.4471 (8)	0.3285 (6)	5.2 (3)
N(3)	0.2784 (6)	-0.0632 (6)	0.1681 (3)	3.2 (2)	C(25)	-0.1208 (9)	0.3551 (8)	0.2789 (5)	4.2 (2)
N(4)	0.2082 (6)	-0.0096 (6)	0.3394 (4)	3.4 (2)					
N(5)	-0.0480 (6)	-0.0083 (5)	0.2853 (3)	3.0 (1)					
C(1)	-0.1987 (8)	0.0656 (8)	0.2850 (5)	3.8 (2)					

^aStarred values denote atoms refined isotropically. Anisotropically refined atoms are given in the form of the isotropic equivalent thermal parameter defined as $4/3[a^2B_{11} + b^2B_{22} + c^2B_{33} + ab(\cos \gamma)B_{12} + ac(\cos \beta)B_{13} + bc(\cos \alpha)B_{23}]$.

terminated spectrophotometrically, and plots of some of the reduced data are shown in Figures 1 and 2.

The plots clearly indicate three equilibria are important over the investigated pH range. At low pHs two overlapping equilibria are observed. The method employed to calculate the pK_a 's does not appear to be applicable when three absorbing species are present. If, however, we ignore for the moment that there are three absorbing species and allow the system to have a squared dependence on $[\text{H}^+]$, then the behavior of the absorbance is as expected for a diprotic acid. As anticipated, no isosbestic points were evident when spectra are recorded over the pH range of 0.5–5.

At pHs higher than 5 a single equilibrium is observed. The fit to the expected pH dependence was excellent, and a single set of isosbestic points was observed throughout the titration. The pK of this reaction is 8.8. In view of the pK_a 's determined for the monosubstituted derivatives (described below) and the conditions used in the preparation, it appears that the last equilibrium corresponds to reaction 8 and equilibrium reaction 5 is not observed.

$\text{Ru}(\text{bpy})_2(\text{HSO}_3)\text{L}^{2+}$. The monosubstituted complex $[\text{Ru}(\text{bpy})_2(\text{H}_2\text{O})(\text{HSO}_3)]\text{PF}_6$ can be prepared by performing the synthesis in 0.1 N H_2SO_4 . The complex, however, appears to be unstable in solution as well as in the solid state. In the solid state, the complex is converted to the aquo complex as indicated by a

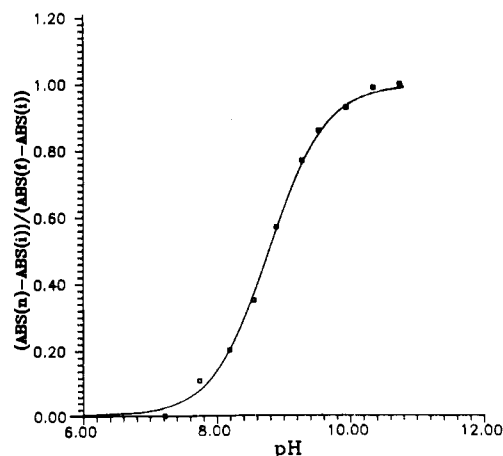


Figure 2. Spectrophotometric titration of $\text{Ru}(\text{bpy})_2(\text{HSO}_3)_2$ over the range of pH 6–12.

gradual darkening of the solid. The solution spectrum of the aged solid confirms the presence of the aquo complex. Approximately 25% conversion takes place in 7 days if the complex is left in an open container.

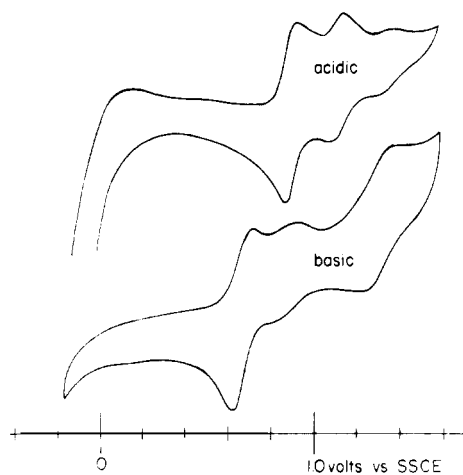


Figure 3. Cyclic voltammograms of $[\text{Ru}(\text{bpy})_2(\text{py})(\text{HSO}_3)]\text{PF}_6$ in acetonitrile with added acid and base.

Solutions of $[\text{Ru}(\text{bpy})_2(\text{H}_2\text{O})(\text{HSO}_3)]\text{PF}_6$ are also unstable and show significant conversion to the aquo complex within a few minutes. The rate of degradation is pH-dependent, and at a pH of 2 or above solutions of the complex cannot be prepared without a majority of the material reverting to the aquo complex. The hydrolysis reaction, however, appears to be catalyzed by hydroquinone-reducible species since the hydrolysis reaction can be reduced to a negligible level by the addition of small amounts of hydroquinone. Solutions in phosphate buffer at pH 7.2 appear to be stable for many hours in the presence of 25 mg of hydroquinone per 100 mL of solution.

$[\text{Ru}(\text{bpy})_2(\text{py})(\text{HSO}_3)]\text{PF}_6$. Complexes with further substitution at the monodentate sites can also be prepared. For example, $[\text{Ru}(\text{bpy})_2(\text{py})(\text{HSO}_3)]\text{PF}_6$ can be prepared by the reaction of $[\text{Ru}(\text{bpy})_2(\text{py})(\text{H}_2\text{O})]\text{PF}_6$ with excess sulfite ion. This appears to be a general reaction scheme and should be applicable to complexes containing other ligands in place of the pyridine.

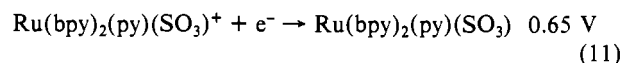
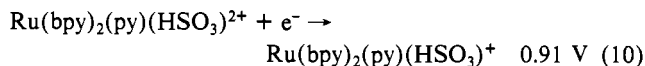
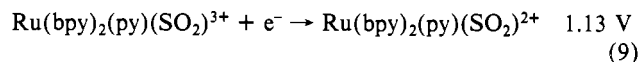
The pyridine-substituted complex is stable as a solid but appears to be susceptible to a catalytic hydrolysis process in solution. Hydroquinone, again, effectively quenches the hydrolysis reaction, and solutions of the complex can be examined over a period of several hours without noticeable loss of bisulfite. Without added hydroquinone, loss of bisulfite is evident within minutes at pHs above 1.5.

Spectrophotometric titrations of the aquo- and pyridine-substituted bisulfite complexes are similar and reveal an interesting feature of these complexes. Specifically, only a single equilibrium is noted over the pH range of 1–7.5. Experimental evidence indicates that this equilibrium is that between bisulfite and sulfite (reaction 13). A shift in the visible absorption maximum from 416 nm in 0.1 N acid to 398 nm in 6 M H_2SO_4 is observed with $\text{Ru}(\text{bpy})_2(\text{HSO}_3)(\text{H}_2\text{O})^+$ and is indicative of the sulfur dioxide/bisulfite equilibrium (reaction 12). These observations are consistent with the fact that only species with coordinated bisulfite are isolated despite the extremely acidic conditions of the preparative scheme.

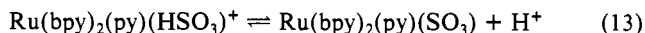
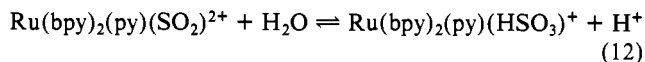
Additional support for the choice of equilibria comes from the cyclic voltammetric study of $\text{Ru}(\text{bpy})_2(\text{HSO}_3)(\text{py})^+$. The cyclic voltammogram is illustrated in Figure 3. The voltammogram of the complex in acetonitrile is disappointingly broad, but three redox processes are evident. The most oxidizing of the three is due to partial decomposition of the complex and the formation of $\text{Ru}(\text{bpy})_2(\text{CH}_3\text{CN})(\text{py})^{2+}$. The addition of a small amount of acid produced a distinct improvement in the voltammogram with three redox reactions clearly evident. If the most oxidizing step is ignored, redox reactions are present with $E_{1/2}$'s of 0.91 and 1.13 V vs SSCE. The redox processes appear to be reversible with peak-to-peak separations of approximately 60 mV each. If 2,6-lutidine is added to a fresh solution, a very different cyclic voltammogram is observed. In this case, three reactions are again observed. The most oxidizing is unchanged as expected, the reaction at 1.13 V is eliminated, and the reaction at 0.91 V is

reduced significantly in magnitude. A new redox process appears at 0.65 V.

The complex electrochemical behavior is readily rationalized with the following assignments of the redox reactions:



The addition of either acid or base shifts the equilibria described by eq 12 and 13. With added acid the formation of the sulfur



dioxide complex is favored and added base produces a predominance of the sulfite complex. Several drops of acid in 2 mL of acetonitrile is insufficient, however, to shift the equilibria completely to the sulfur dioxide form.

The cyclic voltammetry experiments were repeated with more dilute solutions and monitored spectrophotometrically. The results were consistent with the above interpretation. Three acid-base-dependent species were observed with maxima of approximately 400, 440, and 500 nm, respectively. The maxima are approximate since the equilibria could not be shifted sufficiently within the conditions of the experiment to give a spectrum of any one species without interference from the others. Maxima of 402, 440, and 470 nm were obtained in methanol.

One final experimental observation that will be elaborated in another report deals with the chemistry of the trans isomers of the species under discussion. Specifically, *trans*- $[\text{Ru}(\text{bpy})_2(\text{H}_2\text{O})(\text{SO}_2)]\text{PF}_6$ can be isolated as a solid. The complex, however, is extremely reactive and readily reacts with the water in air to form the bisulfite complex.

SO_2 Complexes. The conspicuous absence of sulfur dioxide containing complexes from the extensive ruthenium(II) bipyridine literature appears to be a result of an equilibrium constant that favors the formation of the bisulfite complex even under acidic solutions (i.e., reaction 12). We can attribute this behavior to the strong electrophilic nature of sulfur dioxide when coordinated to the $\text{Ru}^{\text{II}}(\text{bpy})_2$ moiety. This rationalization allows a convenient comparison with other systems that contain the $\text{Ru}^{\text{II}}(\text{bpy})_2$ moiety. For example, the calculated force constant for CO in $\text{Ru}(\text{bpy})_2(\text{CO})_2^{2+}$ is 17.1.⁹ Such a high force constant would place the CO of $\text{Ru}(\text{bpy})_2(\text{CO})_2^{2+}$ among the most electrophilic in the relation published by Darensbourg and Darensbourg¹⁰ and later elaborated by Angelici.¹¹

An analogous trend in electrophilicity may also be evident in the reactions of coordinated NO. For example, the attack of NO^+ by azide ion is rapid when the NO^+ is coordinated to the bis-(bipyridine)ruthenium(II) moiety but does not appear to occur in the case of $\text{Ru}(\text{NH}_3)_3\text{NO}^+$.¹ Bottemley^{1b} has pointed out, however, that this particular case may not be representative of the reactions of coordinated NO in the ammine complexes of Ru(II).

A comparison of the ruthenium(II) centers of bipyridine and tetraammine complexes is instructive at this point. The pK_a 's corresponding to equilibria 12 and 13 for $\text{Ru}(\text{NH}_3)_4(\text{H}_2\text{O})(\text{SO}_2)^{2+}$ are 2.15 and 5.05.¹² In addition, a number of complexes in which the coordinated water has been replaced by various substituted pyridines have been prepared and isolated.² The presence of one good acceptor ligand does not appear to alter the pK_a 's represented by equilibrium 12 sufficiently to prevent the formation of the sulfur

(9) Cotton, F. A.; Kratohanzel, C. S. *J. Am. Chem. Soc.* **1962**, *84*, 4432.
 (10) Darensbourg, D. J.; Darensbourg, M. Y. *Inorg. Chem.* **1970**, *9*, 1691.
 (11) Angelici, R. J. *Acc. Chem. Res.* **1972**, *5*, 335.
 (12) Isied, S.; Taube, H. *Inorg. Chem.* **1974**, *13*, 1545.

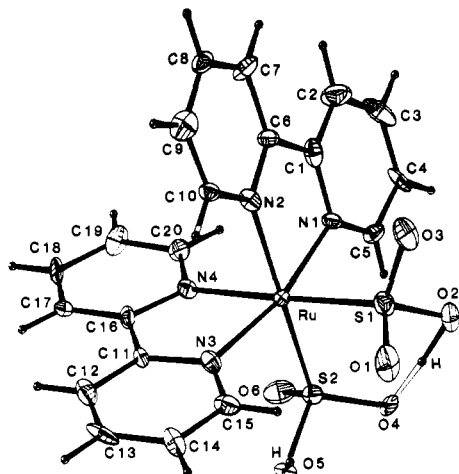


Figure 4. ORTEP diagram (30% ellipsoids) of $[\text{Ru}(\text{bpy})_2(\text{HSO}_3)_2] \cdot \text{H}_2\text{O}$.

dioxide containing complexes as is observed with bis(bipyridine) complexes.

A number of experimental observations, including rates of substitution and redox potentials, clearly indicate that the electron density at the ruthenium(II) bipyridine center is much lower than that in the ammine cases.^{11,13} This is not surprising in view of the fact that bipyridine is a good π acceptor ligand. In the case of coordinated CO it appears that the magnitude of the positive charge on the carbon atom is an important feature in the determination of the electrophilicity, from both a kinetic and thermodynamic standpoint. In the examples provided by Darsenbourg,¹⁰ the positive charge on the carbon atom also correlated with charge at the metal center, as expected. It is not unreasonable to expect coordinated nonmetal oxides, in general, to react similarly and for these reactions to be governed by similar parameters. In this respect, the behavior of coordinated SO_2 , as reflected in a comparison of bipyridine and ammine complexes, is consistent. The magnitude of the difference in electrophilicity of SO_2 coordinated to these two moieties is, however, surprising especially in light of the small difference observed with coordinated NO in these two series of complexes.

Discussion of Structures. Structural determinations of both $\text{Ru}(\text{bpy})_2(\text{HSO}_3)_2$ and $\text{Ru}(\text{bpy})_2(\text{HSO}_3)(\text{py})^+$ have been performed. We know of only one other transition-metal complex containing coordinated HSO_3^- that has been structurally characterized: $\text{Na}_4[\text{Ru}(\text{NH}_3)_2(\text{HSO}_3)_2(\text{SO}_3)_2]$.¹⁴ The structural parameters of the $\text{Ru}(\text{bpy})_2$ fragment are comparable to those parameters in previously published structures containing this molecular fragment.¹⁵ All the Ru-N bonds are as expected, and these show no indication of a trans or cis influence of the bisulfite.

The Ru-S bond distances are similar in both bipyridine complexes as are the S-O bond distances. In both complexes, one

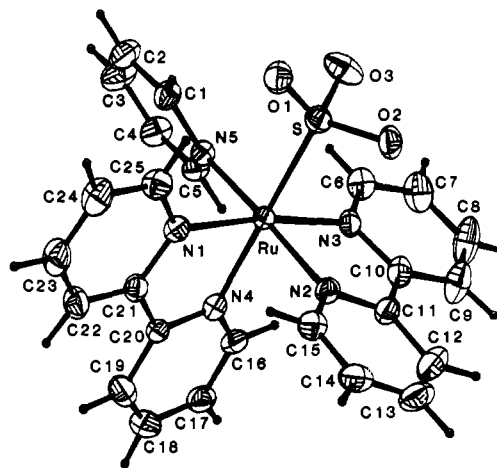


Figure 5. ORTEP diagram (30% ellipsoids) of $[\text{Ru}(\text{bpy})_2(\text{py})(\text{HSO}_3)] \cdot \text{PF}_6 \cdot 3\text{H}_2\text{O}$.

S-O bond is significantly longer than the remaining two and was found to be the hydrogen-bearing oxygen. In $\text{Ru}(\text{bpy})_2(\text{HSO}_3)_2$, there appears to be a hydrogen-bonding interaction between one of the bisulfite hydrogens and the adjacent bisulfite oxygen as indicated in Figure 4. All water molecules and all bisulfite OH groups in these structures are H-bonded to other bisulfite ligands or water molecules; these H-bonds link the complexes of the bis(bisulfite) structure into dimers across a center of symmetry and join the cations of the pyridine-containing complex in chains along the b direction. It should be noted that the elemental analysis of $[\text{Ru}(\text{bpy})_2(\text{HSO}_3)(\text{py})]\text{PF}_6$ indicated that only one water molecule per ruthenium complex was present in the sample. We attribute this discrepancy to the differences in conditions under which the analytical sample was obtained. The sample was precipitated rapidly from solution and then dried by washing with 2-propanol and ethyl ether.

A comparison of the Ru-S and S-O bond distances in these complexes and the ammine complex mentioned above is interesting in light of the previous comparison of electrophilicity. In the ammine complex, both the Ru-S and S-O bond distances are, on the average, longer than those of the bipyridine complexes. While these bonding interactions represent only one energy component of the equilibrium between bound SO_2 and HSO_3^- , the trend is consistent with the electrophilicity arguments.

Acknowledgment. We thank the donors of the Petroleum Research Fund, administered by the American Chemical Society, the National Science Foundation, and the State of Arkansas for support of this research.

Registry No. *cis*- $\text{Ru}(\text{bpy})_2\text{Cl}_2$, 19542-80-4; *cis*- $[\text{Ru}(\text{bpy})_2(\text{py})\text{Cl}]\text{PF}_6$, 36413-31-7; *cis*- $[\text{Ru}(\text{bpy})_2(\text{HSO}_3)_2] \cdot \text{H}_2\text{O}$, 116663-17-3; *cis*- $[\text{Ru}(\text{bpy})_2(\text{HSO}_3)(\text{H}_2\text{O})]\text{PF}_6$, 116663-19-5; *cis*- $[\text{Ru}(\text{bpy})_2(\text{HSO}_3)(\text{py})]\text{PF}_6 \cdot \text{H}_2\text{O}$, 116663-21-9; *cis*- $[\text{Ru}(\text{bpy})_2(\text{HSO}_3)_2]$, 116663-27-5; $\text{Ru}(\text{bpy})_2(\text{SO}_2)(\text{HSO}_3)$, 116669-11-5; $\text{Ru}(\text{bpy})_2(\text{HSO}_3)(\text{SO}_3)$, 116663-26-4; $\text{Ru}(\text{bpy})_2(\text{SO}_3)_2$, 116663-23-1; $\text{Ru}(\text{bpy})_2(\text{SO}_2)(\text{H}_2\text{O})$, 116663-24-2; $\text{Ru}(\text{bpy})_2(\text{SO}_3)(\text{H}_2\text{O})$, 116663-18-4; $\text{Ru}(\text{bpy})_2(\text{SO}_2)(\text{py})$, 116663-25-3; $\text{Ru}(\text{bpy})_2(\text{SO}_3)(\text{py})$, 116663-20-8; $[\text{Ru}(\text{bpy})_2(\text{py})(\text{HSO}_3)]\text{PF}_6$, 116663-22-0.

Supplementary Material Available: Tables SI and SII, listing crystallographic data and the anisotropic thermal parameters (4 pages); tables of calculated and observed structure factors (61 pages). Ordering information is given on any current masthead page.

- (13) Allen, L. R.; Craft, P. P.; Durham, B.; Walsh, J. *Inorg. Chem.* **1987**, *26*, 53.
- (14) Johnson, D. A.; Jeter, D. Y.; Cordes, A. W. *Acta Crystallogr.* **1987**, *C43*, 2001.
- (15) Durham, B.; Wilson, S. R.; Hodgson, D. J.; Meyer, T. J. *J. Am. Chem. Soc.* **1980**, *102*, 600.
- (16) *International Tables for X-Ray Crystallography*; Kynoch: Birmingham, England, 1974.